

Molecular photoelectron momentum and angular distributions of N_2 molecules by ultrashort attosecond laser pulses

Si-Qi Zhang(张思琪), Qi Zhen(甄琪), Zhi-Jie Yang(杨志杰), Jun Zhang(张军), Ai-Hua Liu(刘爱华), Kai-Jun Yuan(元凯军), Xue-Shen Liu(刘学深), and Jing Guo(郭静)

Citation: Chin. Phys. B, 2021, 30 (**4**): 043201. DOI: 10.1088/1674-1056/abca22
Journal homepage: http://cpb.iphy.ac.cn; http://iopscience.iop.org/cpb

What follows is a list of articles you may be interested in

Generation of non-integer high-order harmonics and significant enhancement of harmonic intensity

Chang-Long Xia(夏昌龙), Yue-Yue Lan(兰悦跃), and Xiang-Yang Miao(苗向阳)
Chin. Phys. B, 2021, 30 (**4**): 043202. DOI: 10.1088/1674-1056/abd389

Probing time delay of strong-field resonant above-threshold ionization

Shengliang Xu(徐胜亮), Qingbin Zhang(张庆斌), Cheng Ran(冉成), Xiang Huang(黄湘), Wei Cao(曹伟), and Peixiang Lu(陆培祥)
Chin. Phys. B, 2021, 30 (**1**): 013202. DOI: 10.1088/1674-1056/abc7a5

Ultrafast photoionization of ions and molecules by orthogonally polarized intense laser pulses: Effects of the time delay

Si-Qi Zhang(张思琪), Zhi-Jie Yang(杨志杰), Zhi-Xian Lei(雷志仙), Wei Feng(冯伟), Sheng-Peng Zhou(周胜鹏), Kai-Jun Yuan(元凯军), Xue-Shen Liu(刘学深), and Jing Guo(郭静)
Chin. Phys. B, 2021, 30 (**1**): 013201. DOI: 10.1088/1674-1056/abb30c

Resonance-enhanced two-photon ionization of hydrogen atom in intense laser field investigated by Bohmian-mechanics

Yang Song(宋阳), Shu Han(韩姝), Yu-Jun Yang(杨玉军), Fu-Ming Guo(郭福明), Su-Yu Li(李苏宇)
Chin. Phys. B, 2020, 29 (**9**): 093204. DOI: 10.1088/1674-1056/aba09e

Relative phase-dependent two-electron emission dynamics with two-color circularly polarized laser fields

Tong-Tong Xu(徐彤彤), Lian-Lian Zhang(张莲莲), Zhao Jin(金钊), Wei-Jiang Gong(公卫江)
Chin. Phys. B, 2020, 29 (**9**): 093202. DOI: 10.1088/1674-1056/ab928c

---

Molecular photoelectron momentum and angular distributions of N_2 molecules by ultrashort attosecond laser pulses*

Si-Qi Zhang(张思琪), Qi Zhen(甄琪), Zhi-Jie Yang(杨志杰), Jun Zhang(张军), Ai-Hua Liu(刘爱华), Kai-Jun Yuan(元凯军), Xue-Shen Liu(刘学深), and Jing Guo(郭静)†

Institute of Atomic and Molecular Physics, Jilin University, Changchun 130012, *China*

(Received 10 September 2020; revised manuscript received 3 November 2020; accepted manuscript online 13 November 2020)

The ultrafast photoionization dynamics of N_2 molecules by x-ray/XUV laser pulses is investigated. The molecular frame photoelectron momentum distributions (MF-PMDs) and the molecular frame photoelectron angular distributions (MF-PADs) are obtained by numerically solving 2D time-dependent Schrödinger equations within the single-electron approximation (SEA) frame. The results show that the molecular photoionization diffraction appears in 5 nm laser fields. However, when the laser wavelength is 30 nm, the molecular photoionization diffraction disappears and the MF-PMDs show four-lobe pattern. The ultrafast photoionization model can be employed to describe the MF-PMDs and MF-PADs of N_2 molecules.

Keywords: N_2 molecules, molecular frame photoelectron momentum distributions, ultrafast photoionization model

PACS: 32.80.Rm, 32.80.Fb, 42.50.Hz, 42.65.Re **DOI:** 10.1088/1674-1056/abca22

1. Introduction

With the rapid advances of ultrashort laser technology,[1–3] electronic dynamics in atoms and molecules on attosecond (10^{-18} s) time scales has attracted great attention.[4–12] Recently, attosecond pulses with a duration of 43 as have been achieved by Gaumnitz *et al.*,[13] which can track electronic motion. Time-resolved photoelectron momentum and angular distributions based on the pump-probe techniques has been used as an efficient tool to investigate molecular reaction dynamics.[14–16] A transition between the ground state and the excited state of the target is initiated by the ultrafast pump laser pulse, and the dynamics process of the target is monitored by probe pulse.

Cohen and Fano[17] firstly suggested the interference of electron wavepackets in a diatomic molecule in perturbative single-photon ionization, and then Walter and Briggs modeled the interference of electron wavepackets in molecules.[18] Zuo *et al.* have extended such interference of electron wavepackets to nonperturbative regime.[19] Utilizing the ultrafast laser pulses to the molecules can induce the laser-induced electron interference and laser-induced electron diffraction (LIED), which is applied as an effective tool for imaging molecular orbitals.

Molecular photoelectron diffraction can imagine the time-resolved molecular dynamics.[20–23] Yuan *et al.*[24] theoretically studied triatomic molecular photoelectron diffraction by circularly x-ray laser pulses, they found that molecular photoelectron diffraction patterns show dependence on the symmetry of the molecular orbitals. Attosecond electron coherences have been tracked by photoelectron spectra in the x-ray region, which can allow one to monitor attosecond electron migration in atoms and molecules.[25] The photoelectron diffraction patterns in photoelectron spectra encode information about the molecular intrinsic properties including the orbital symmetry of the molecules. Some researchers investigated the dependence of the geometries and orbital structures on the photoelectron diffraction patterns of the N_2 and CO_2 molecules in few-cycle laser pulses.[26–28] Experimentally, the diffraction patterns of O_2 and N_2 molecules were reported by Meckel *et al.* in 2008.[29] For experiments, photoelectron momentum distributions (PMDs) and photoelectron angular distributions (PADs) are usually detected in the laboratory frame. Some researches[30,31] have explored the connection between PADs measured in the molecular frame and PADs measured in the laboratory frame.

Recently, the researches about the molecular ultrafast dynamics have been achieved with the single-electron approximation (SEA) frame,[27,32–34] which has been used to study the ionization dynamics of the multi-electron molecules by intense ultrashort linearly polarized laser pulses. Int the present study, we extend the SEA frame for studying photonionization of the diatomic N_2 molecules to x-ray/XUV regions. The molecular frame photoelectron momentum distributions (MF-PMDs) and molecular frame photoelectron angular distributions (MF-PADs) of N_2 molecules are investigated in circularly polarized attosecond laser fields.

The paper is organized as follows: In Section 2 we describe the numerical method for solving TDSE of the aligned

*Project supported by the National Natural Science Foundation of China (Grant Nos. 12074146, 11974007, 12074142, 11904122, 91850114, and 11774131) and the Natural Science Foundation of Jilin Province of China (Grant No. 20180101225JC).

†Corresponding author. E-mail: gjing@jlu.edu.cn

© 2021 Chinese Physical Society and IOP Publishing Ltd

N_2 molecules within the SEA frame. The results of numerical calculation and theoretical prediction are discussed in Section 3. In Section 4, we summarize our findings. Atomic units (a.u.) ($e = \hbar = m_e = 1$) are adopted unless specifically stated.

2. Numerical methods

The electron dynamics of the N_2 molecules within the static nuclei and SEA frame is investigated by solving the two-dimensional (2D) time-dependent Schrödinger equations (TDSEs) as follows:

$$\mathrm{i}\frac{\partial\psi(\boldsymbol{r},t)}{\partial t} = \left[\frac{\boldsymbol{p}^2}{2} + V(\boldsymbol{r}) + V_{\mathrm{L}}(\boldsymbol{r},t)\right]\psi(\boldsymbol{r},t), \tag{1}$$

where $\boldsymbol{p}$ is the photoelectron momentum, and the potential of the N_2 molecules has the form[27,32]

$$V(\boldsymbol{r}) = -\sum_j \frac{Z_j^{\infty} + (Z_j^0 - Z_j^{\infty})\exp(-\boldsymbol{r}_j^2/\sigma_j^2)}{\sqrt{\boldsymbol{r}_j^2 + a_j^2}}. \tag{2}$$

The parameters used in the potential of N_2 molecules are same as those in Ref. [32].

The imaginary-time propagation method has been used to obtain the initial wavefunction of N_2 molecules, the N_2 molecule is aligned along the x axis, $R_{\mathrm{N-N}} = 2.08$ a.u. is the equilibrium internuclear distance.[27,35] The initial state of the highest occupied molecular orbital (HOMO) for N_2 molecules is shown in Fig. 1. One sees that the N_2 molecule has three nodes mainly located along the molecular $\boldsymbol{R}$ axis with the σ_g symmetry. The ionization potential is $I_p = 15.6$ eV.[32]

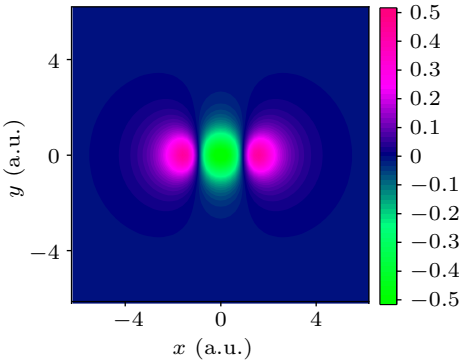


Fig. 1. The HOMO orbital of the N_2 molecule.

The interaction between the laser pulse and the electron of N_2 molecule is $V_{\mathrm{L}}(\boldsymbol{r},t) = \boldsymbol{r}\cdot\boldsymbol{E}(t)$, $\boldsymbol{E}(t)$ is field vector in the (x, y) polarization plane, the circularly polarized laser pulse in our simulation is

$$\begin{aligned}\boldsymbol{E}(t) &= E_x(t)\hat{\boldsymbol{e}}_x + E_y(t)\hat{\boldsymbol{e}}_y \\ &= E_0 f(t)\left[\cos(\omega t)\hat{\boldsymbol{e}}_x + \sin(\omega t)\hat{\boldsymbol{e}}_y\right].\end{aligned} \tag{3}$$

The laser intensity is $E_0 = 5.34\times10^{-2}$ a.u. ($I_0 = 1\times10^{14}$ W/cm^2); ω is the laser frequency, and $\hat{\boldsymbol{e}}_{x/y}$ is the polarization direction of the laser. A smooth pulse envelope $f(t) = \sin^2(\pi t/T)$ of duration $T = 10T_0$ is used, and one optical cycle (o.c.) is $T_0 = 2\pi/\omega$.

The second-order split-operator method is used in our calculation to obtain the wavefunction propagation in time,[36,37]

$$\begin{aligned}\psi(\boldsymbol{r},t+\Delta t) &= \mathrm{e}^{-\mathrm{i}(\frac{p^2}{4})\Delta t}\,\mathrm{e}^{-\mathrm{i}[V(\boldsymbol{r})+V_{\mathrm{L}}(\boldsymbol{r},t)]\Delta t}\,\mathrm{e}^{-\mathrm{i}(\frac{p^2}{4})\Delta t}\,\psi(\boldsymbol{r},t) \\ &\quad + O(\Delta t^3).\end{aligned} \tag{4}$$

The total length of spatial grid is 204.8 a.u. The wavefunction is multiplied by a mask function of the form $\cos^{1/8}$ at each time step to suppress unphysical reflection from the boundary, the mask function $M(\boldsymbol{r})$ is same as that in Ref. [32], and the absorber domain is from 75 a.u. to 102.4 a.u. The ionized part is recorded as $[1-M(\boldsymbol{r})]\psi(\boldsymbol{r},t)$, and $r = \sqrt{x^2+y^2}$. The MF-PMDs are obtained by Fourier transformation from the time-dependent electronic wavefunction.[38] The MF-PADs are obtained from the MF-PMDs.

3. Results and discussion

We focus on the photoionization process of the N_2 molecules to describe the effect of wavelength and rotation of laser field on MF-PMDs and MF-PADs by high-frequency soft x-ray and XUV laser pulses. We only study the MF-PMDs and the MF-PADs around the energy $\omega - I_p$, and other excited states of the system are neglected.

The MF-PMDs and MF-PADs are presented by a circularly polarized x-ray laser pulse with the wavelength $\lambda = 5$ nm ($\omega = 9.11$ a.u.) in Fig. 2. The duration is chosen as $T = 10T_0$, and $T_0 = 2\pi/\omega$. From Fig. 2 one sees that the MF-PMDs and MF-PADs are mainly localized along the p_x direction. The corresponding photoelectron momentum is about $p = 4.1$ a.u., two radiation peaks at angles 0° and 180° with large amplitudes appear, and four radiation peaks at angles $n\times180°\pm62°$ ($n = 0$, 1) with small amplitudes also appear. The photoelectron diffraction occurs in the MF-PMDs and MF-PADs. The photoelectron energy is much larger than the ionization potential of the molecules, i.e., $\omega \gg I_p$, the molecular Coulomb potential has little influence on the electron with larger momentum. Thus, the photoelectron diffractions in the MF-PMDs and MF-PADs are determined by the symmetry of the N_2 molecule.

We use the ultrafast photoionization model based on the δ-function[19,32,39] to interpret the photoelectron distribution. The wavefunction of HOMO for the N_2 molecules can be expressed as $\psi_0(\boldsymbol{r}) = [\psi_{2p_x}(\boldsymbol{r}-\boldsymbol{R}_{\mathrm{L,N}}) - \psi_{2p_x}(\boldsymbol{r}-\boldsymbol{R}_{\mathrm{R,N}})]/\sqrt{2}$. Then, we get the total transition amplitude

$$\mathcal{F}_{N_2}(\boldsymbol{p}) \propto |\sqrt{2}(\boldsymbol{n}\cdot\boldsymbol{e})\sin(\boldsymbol{P}\cdot\boldsymbol{R}_{\mathrm{N-N}}/2)|^2\psi_{2p_x}^2(|\boldsymbol{p}|), \tag{5}$$

where $\boldsymbol{e}$ is the vector unit of the laser polarization vector, $\boldsymbol{n}$ is unit vector of the transition dipole, and $\boldsymbol{P} = \boldsymbol{p} + \boldsymbol{E}$. The delta-function pulse in the ultrafast photoionization model is

used to shift the photoelectron distributions of molecular orbitals by the momentum of the laser field vector $\boldsymbol{E}$. Thus the photoelectron momentum distributions in our simulation can be written as

$$\mathcal{F}_{N_2}(\boldsymbol{p}) \propto |\sqrt{2}(\boldsymbol{n}\cdot\boldsymbol{e})\sin[\boldsymbol{P}\cdot\boldsymbol{R}_{N-N}/2)]\psi_{2p_x}(|\boldsymbol{p}|)|^2. \quad (6)$$

The negligible ponderomotive energy $U_p \ll I_p$ and $E \ll p$, therefore the laser field $\boldsymbol{E}$, can be ignored and then we can obtain $\boldsymbol{p} \approx \boldsymbol{P}$. Moreover, the shape of the wavefunction of the ψ_{2p_x} orbital is proportional to the function of $\cos\theta$. The MF-PMDs and MF-PADs can be expressed as

$$\mathcal{F}_{N_2}(\boldsymbol{p}) \sim |\cos\theta \sin[pR_{N-N}\cos(\theta)/2]|^2, \quad (7)$$

where θ defines the angle between the photoelectron momentum $\boldsymbol{p}$ and the x axis.

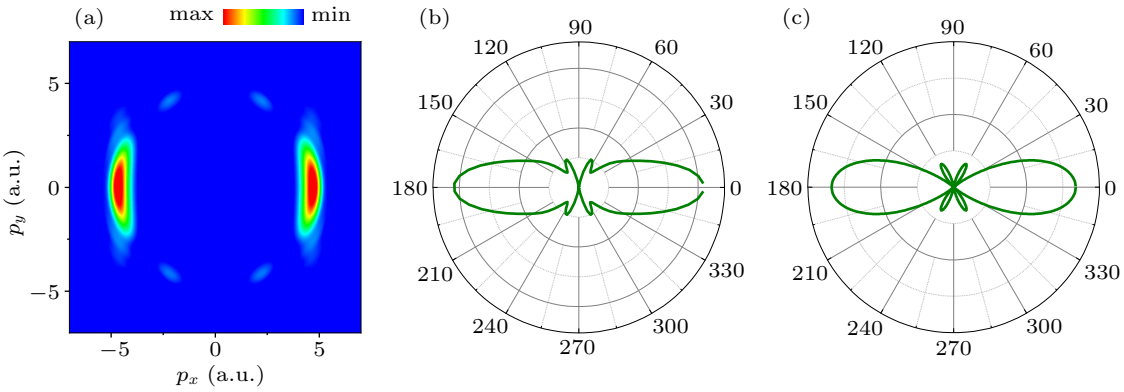


Fig. 2. Molecular-frame photoelectron diffraction patterns of the N_2 molecules at equilibrium internuclear distance $R_{N-N} = 2.08$ a.u. by a circularly polarized laser pulse at $\lambda = 5$ nm ($\omega = 9.11$ a.u.): (a) the MF-PMDs, and (b) the MF-PADs obtained by integrating over energy, (c) theoretical prediction obtained from Eq. (7).

According to the energy conservation, the photoelectron momentum and the de Broglie wavelength are $p_{N_2} = \sqrt{2(\omega - I_p)} = 4.13$ a.u. and $\lambda_{N_2} = 2\pi/p_{N_2} = 1.52$ a.u. in 5 nm laser fields. For the N_2 molecule at equilibrium internuclear distance, $\lambda_{N_2} < R_{N-N}$, so the diffraction pattern appears in the photoelectron distributions.[16] We also present the theoretical prediction in Eq. (7) obtained from the ultrafast photoionization model in Fig. 2(c). Six radiation peaks with different amplitudes are same as the MF-PADs in Fig. 2(b), the angles of the radiation peaks predicted from ultrafast photoionization model are in good agreement with those of the TDSE simulations.

When the photon energy is slightly larger than the molecular ionization potential, $\omega > I_p$, the electron with lower momentum is inclined to be influenced by the molecular Coulomb potential in the photoionization process. Thus the MF-PMDs and MF-PADs can be strongly influenced by the Coulomb effect. We next consider the photoionization process of N_2 molecules by an XUV pulse with the wavelength $\lambda = 30$ nm. In Fig. 3 we show the MF-PMDs and MF-PADs of the N_2 molecules by a counter-clockwise circularly polarized laser pulse at wavelength $\lambda = 30$ nm ($\omega = 1.52$ a.u.), which is different from the results in Fig. 2. The duration is $T = 10T_0$, and $T_0 = 2\pi/\omega$. Therefore, the patterns of the MF-PMDs and MF-PADs depend on the wavelengths. The momentum of the photoelectron is $p'_{N_2} = 1.38$ a.u. and de Broglie wavelength of the photoelectron is $\lambda'_{N_2} = 4.55$ a.u. for N_2 molecules at $\lambda = 30$ nm. Obviously, diffraction pattern in the photoelectron distributions disappear because $\lambda'_{N_2} > R_{N-N}$. The MF-PMDs of N_2 molecules by a counter-clockwise circularly polarized laser pulse have four components, and the strongest intensity of the four components are localized at 35°, 140°, 213°, 320°, and the MF-PADs have six radiation peaks, four radiation peaks with large amplitudes are localized at 35°, 140°, 213°, 320° and two radiation peaks with small amplitudes are localized at 82°, 262°. One sees that rotations of the MF-PMDs and MF-PADs appear of N_2 molecules by a clockwise circularly polarized laser pulse in Fig. 3(b). The MF-PMDs in Fig. 3(a) and the MF-PMDs in Fig. 3(b) show mirror symmetry, and the MF-PADs is the same as the MF-PMDs. Due to the fact that the Coulomb effects have influence on the molecular photoionization, the ultrafast photoionization models are modified by using the angle-resolved ionization probability. The ionization probability in different direction by a linearly polarized laser pulse with the wavelength $\lambda = 30$ nm is calculated. The other parameters are the same as those in Fig. 2. The ionization probability of the N_2 molecule is a function of $sin\theta$, therefore the modified MF-PMDs and MF-PADs can be expressed as

$$\mathcal{F}_{N_2}(\boldsymbol{p}) \sim |\sin\theta\cos\theta \sin[pR_{N-N}(\cos\theta)/2]|^2. \quad (8)$$

In Fig. 3(c), the results are obtained from the modified ultrafast photoionization models predicted in Eq. (8) at the momentum $p'_{N_2} = 1.38$ a.u. It is found that the predicted results of the N_2 molecules exhibit four angular nodes at $\pm 38°$ and $\pm 142°$, which are in agreement with the TDSE results in Figs. 3(a) and 3(b).

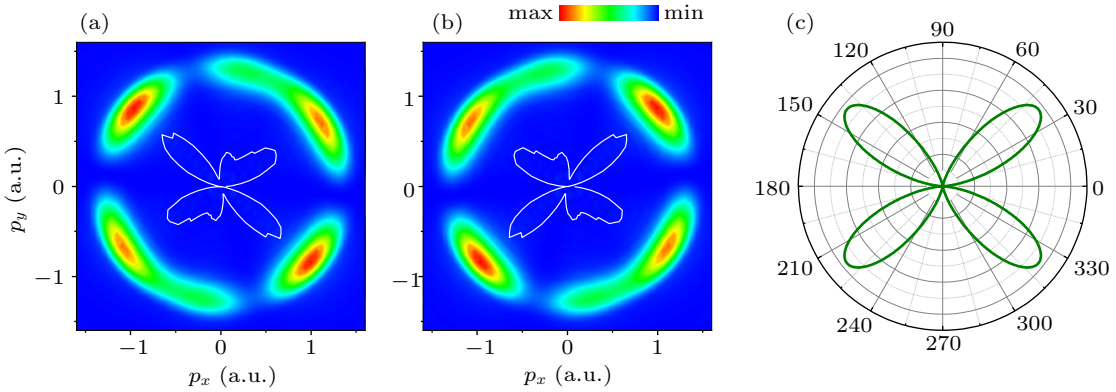


Fig. 3. Molecular-frame photoelectron momentum distribution of the N_2 molecules by (a) a counter-clockwise and (b) a clockwise circularly polarized laser pulse at $\lambda = 30$ nm ($\omega = 1.52$ a.u.). (c) theoretical prediction obtained from the Eq. (8).

To further understand the rotation direction of the MF-PMDs and MF-PADs of N_2 molecules in the XUV laser field, we present the MF-PMDs and MF-PADs by linearly polarized laser pulses with the wavelength $\lambda = 30$ nm in Fig. 4. The intensity and duration of the laser are the same as those in Fig. 3. The MF-PMDs and MF-PADs in the parallel linearly polarized laser pulse for N_2 molecules are shown in Fig. 4(a), four components of the MF-PMDs for N_2 molecules are distributed in four quadrants respectively, and the intensities of the four components are identical. The distributions cover ranges 28°–79°, 94°–147°, 214°–266°, and 283°–335°. The MF-PADs have four radiation peaks localized at 56°, 123°, 236°, 303°. The MF-PMDs and MF-PADs of the N_2 molecule in a perpendicular linearly polarized laser fields are shown in Fig. 4(b), the MF-PMDs have six components, and four components with stronger intensity are distributed in four quadrants respectively, the distributions cover the ranges 9°–58°, 118°–173°, 188°–239°, and 305°–348°. However two components with weaker intensity are located along the y axis, and the distributions cover the range from 76° to 99° along the upper half of the y axis and the range from 261° to 283° along the bottom half of the y axis. The six radiation peaks of the MF-PADs are localized at 33°, 90°, 146°, 213°, 270°, 328°. The MF-PMDs and MF-PADs of N_2 molecules by circularly polarized laser pulses with wavelength $\lambda = 30$ nm are shown in Fig. 3, the distributions of the MF-PMDs have four components, and the distributions cover the range from 9° to 96° in the first component, the range from 113° to 165° in the second component, the range from 184° to 275° in the third component, and the range from 296° to 348° in the fourth component. Six radiation peaks of the MF-PADs are localized at 35°, 82°, 140°, 213°, 262°, and 320°. Thus the MF-PMDs for N_2 molecules in circularly polarized laser fields in Fig. 3 are superpositions of the MF-PMDs in both parallel and perpendicular linearly polarized laser fields[40] and the case of the MF-PADs is the same as the MF-PMDs. The rotation direction depends on the helicity of the laser field.[41,42]

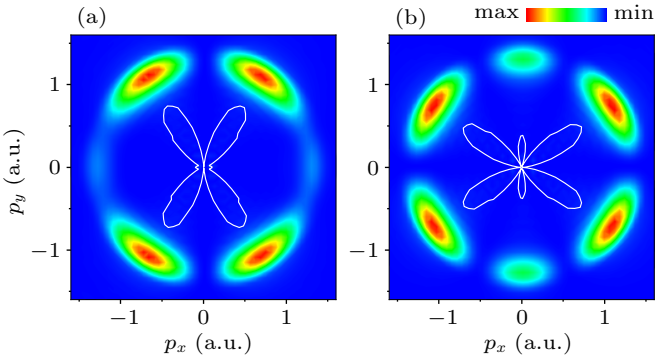


Fig. 4. The MF-PMDs and MF-PADs of the N_2 molecule by linearly polarized laser pulses at $\lambda = 30$ nm ($\omega = 1.52$ a.u.): (a) parallel linear polarization (parallel to the x molecular axis), (b) perpendicular linear polarization (perpendicular to the x molecular axis).

For further understanding the facts that the MF-PMDs by the circularly polarized laser pulse are superpositions of the linearly parallel and perpendicular polarized cases, the superpositions of MF-PMDs for the N_2 molecule in parallel linearly polarized fields and perpendicular linearly polarized fields are shown in Fig. 5. The counter-clockwise circularly polarized laser pulse is the sum of parallel linearly polarized pulse and perpendicular linearly polarized pulse, thus we add up the wavefunction of final states in coordinate space in the parallel linearly polarized fields and perpendicular linearly polarized fields, and transform the superimposed wavefunction in coordinate space to the momentum $\boldsymbol{p}$ space, the superpositions for the case of the counter-clockwise circularly polarized laser pulses is shown in Fig. 5(a), which is in agreement with the numerical result in Fig. 3(a). Similarly, the clockwise circularly polarized laser pulse is the subtraction of parallel linearly polarized pulse and perpendicular linearly polarized pulse, thus we subtract the wavefunction of final states in coordinate space in the parallel linearly polarized fields and perpendicular linearly polarized fields, and transform the superimposed wavefunction in coordinate space to the momentum $\boldsymbol{p}$ space, the superpositions for the case of the clockwise circularly polarized laser pulses is shown in Fig. 5(b), which is in agreement with the numerical result in Fig. 3(b).

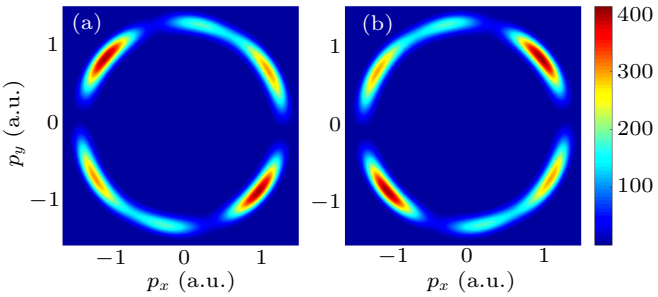


Fig. 5. The superpositions of MF-PMDs for the N_2 molecule in parallel linearly polarized fields and perpendicular linearly polarized fields: (a) the superpositions for the case of the counter-clockwise circularly polarized laser pulses, (b) the superpositions for the case of the clockwise circularly polarized laser pulses.

4. Conclusions

In summary, we have studied the ultrafast photoionization process of N_2 molecules by numerically solving 2D TDSE within the frozen-nuclei and SEA frame. The photoelectron momentum and angular distributions of the HOMO electronic state for N_2 molecules are presented in circularly polarized laser fields. Numerical results show that the wavelengths of the laser pulses have influence on the structure of the MF-PMDs and the MF-PADs. Diffraction patterns in the photoelectron distributions are induced by a soft x-ray circularly polarized laser at $\lambda = 5$ nm, the ultrafast photoionization model can be employed to interpret the MF-PMDs and MF-PADs.[19] The molecular Coulomb potential has little influence on the electron with larger momentum at x-ray high frequency regions. For comparison, we present the MF-PMDs and MF-PADs by an XUV laser pulse at $\lambda = 30$ nm, in this case, the electron with lower momentum is inclined to be influenced by the molecular Coulomb potential in the photoionization process, thus the Coulomb effect cannot be ignored. The angle-resolved ionization probability is used to modify the ultrafast photoionization model, the modified ultrafast photoionization model can be employed to interpret the MF-PMDs and MF-PADs. It is also found that changing the sign of the helicity will lead to the rotation of the MF-PMDs and MF-PADs, and the rotation direction depends on the helicity of the circularly polarized laser pulses. In addition, we also present the MF-PMDs and MF-PADs by both parallel and perpendicular linearly polarized laser pulses with the wavelength $\lambda = 30$ nm, and the MF-PMDs by the circularly polarized laser pulse are superpositions of the MF-PMDs for the linearly parallel and perpendicular polarized cases.

References

[1] Brabec T and Krausz F 2000 *Rev. Mod. Phys.* **72** 545
[2] Krausz F 2009 *Rev. Mod. Phys.* **81** 163
[3] Goulielmakis E, Loh Z, Wirth A, Santra R, Rohringer N, Yakovlev V S, Zherebtsov S, Pfeifer T, Azzeer A M, Kling M F, Leone S R and Krausz F 2010 *Nature* **466** 739
[4] Xia C L, Lan Y Y, Li Q Q and Miao X Y 2019 *Chin. Phys. B* **28** 103203
[5] Zhao X, Wei H, Wu Y and Lin C D 2017 *Phys. Rev. A* **95** 043407
[6] Liang H J, Fan X, Feng S, Shan L Y, Gao Q H, Yan B, Ma R, Xu H F and Ding D J 2019 *Chin. Phys. B* **28** 094211
[7] Li M, Zhang G Z, Ding X and Yao J Q 2019 *Chin. Phys. Lett.* **36** 063201
[8] Zhao Xi, Wei H, Yu W W and Lin C D 2018 *Phys. Rev. A* **98** 053404
[9] Shao J, Zhang C P, Jia J C, Ma J L and Miao X Y 2019 *Chin. Phys. Lett.* **36** 054203
[10] Yang W, Zhang H, Lin C, Xu J, Sheng Z, Song X, Hu S and Chen J 2016 *Phys. Rev. A* **94** 043419
[11] Gong X, Lin C, He F, Song Q, Lin K, Ji Q, Zhang W, Ma J, Lu P, Liu Y, Zeng H, Yang W and Wu J 2017 *Phys. Rev. Lett.* **118** 143203
[12] Song X, Shi G, Zhang G, Xu J, Lin C, Chen J and Yang W 2018 *Phys. Rev. Lett.* **121** 103201
[13] Gaumnitz T, Jain A, Pertot Y, Huppert M, Jordan I, Ardana-Lamas F and Wörner H J 2017 *Opt. Express* **25** 27506
[14] Zewail A H 2000 *J. Phys. Chem. A* **104** 5660
[15] Stolow A, Bragg A E and Neumark D M 2004 *Chem. Rev.* **104** 1719
[16] Reid K L 2008 *Int. Rev. Phys. Chem.* **27** 607
[17] Cohen H D and Fano U 1966 *Phys. Rev.* **150** 30
[18] Walter M and Briggs J 1999 *J. Phys. B* **32** 2487
[19] Zuo T, Bandrauk A D and Corkum P B 1996 *Chem. Phys. Lett.* **259** 313
[20] Pullen M G, Wolter B, Le A T, Baudisch M, Hemmer M, Senftleben A, Schröter C D, Ullrich J, Moshammer R, Lin C D and Biegert J 2015 *Nat. Commun.* **6** 7262
[21] Ito Y, Wang C, Le A T, Okunishi M, Ding D, Lin C D and Ueda K 2016 *Struct. Dyn.* **3** 034303
[22] Nguyen-Dang T T, Peters M, Viau-Trudel J, Couture-Bienvenue E, Puthumpally-Joseph R, Charron E and Atabek O 2017 *Mol. Phys.* **115** 1934
[23] Vrakking M J J 2009 *Physics* **2** 72
[24] Yuan K J and Bandrauk A D 2020 *Phys. Chem. Chem. Phys.* **22** 325
[25] Yuan K J and Bandrauk A D 2020 *J. Phys. B: At. Mol. Opt. Phys.* **53** 064002
[26] Peters M, Nguyen-Dang T T, Cornaggia C, Saugout S, Charron E, Keller A and Atabek O 2011 *Phys. Rev. A* **83** 051403
[27] Peters M, Nguyen-Dang T, Charron E, Keller A and Atabek O 2012 *Phys. Rev. A* **85** 053417
[28] Li Y, Qin M, Zhu X, Zhang Q, Lan P and Lu P 2015 *Opt. Express* **23** 10687
[29] Meckel M, Comtois D, Zeidler D, Staudte A., Pavii D, Bandulet H C, Ppin H, Kieffer J C, Drner R, Villeneuve D M and Corkum P B 2008 *Science* **320** 1478
[30] Reid K L 2003 *Ann. Rev. Phys. Chem.* **54** 397
[31] Underwood J G and Reid K L 2000 *J. Chem. Phys.* **113** 1067
[32] Zhang S Q, Yang Z J, Lei Z X, Feng W, Zhou S P, Yuan K J, Liu X S and Guo J 2020 *Chin. Phys. B*
[33] Spiewanowski M D and L B Madsen 2014 *Phys. Rev. A* **89** 043407
[34] Yu C and Madsen L B 2017 *Phys. Rev. A* **95** 063407
[35] Rolles D 2005 *Nature* **437** 711
[36] Bandrauk A D and Shen H 1993 *J. Chem. Phys.* **99** 1185
[37] Bandrauk A D and Lu H 2013 *J. Theor. Comput. Chem.* **12** 1340001
[38] Zhang H D, Ben S, Xu T T, Song K L, Tian Y R, Xu Q Y, Zhang S Q, Guo J and Liu X S 2018 *Phys. Rev. A* **98** 013422
[39] Yuan K J and Bandrauk A D 2014 *J. Phys.: Conf. Ser* **497** 012014
[40] Horner D A, Miyabe S, Rescigno T N and McCurdy C W 2008 *Phys. Rev. Lett.* **101** 183002
[41] Yuan K J, Chelkowski S and Bandrauk A D 2014 *Chem. Phys. Lett.* **592** 334
[42] Yuan K J, Chelkowski S and Bandrauk A D 2015 *J. Chem. Phys.* **142** 144304